Computationally Designed Peptide Inhibitors of Protein−Protein Interactions in Membranes[†]

Gregory A. Caputo,[‡,§] Rustem I. Litvinov,[‡] Wei Li,[||] Joel S. Bennett,[||] William F. DeGrado,[‡] and Hang Yin*[,⊥]

Department of Chemistry and Biochemistry, University of Colorado, Boulder, Colorado 80309-0215, and Department of Cell and Developmental Biology, Department of Medicine, Hematology-Oncology Division, and Department of Biochemistry and Biophysics, University of Pennsylvania School of Medicine, Philadelphia, Pennsylvania 19104

Received April 18, 2008; Revised Manuscript Received May 29, 2008

ABSTRACT: We recently reported a computational method (CHAMP) for designing sequence-specific peptides that bind to the membrane-embedded portions of transmembrane proteins. We successfully applied this method to design membrane-spanning peptides targeting the transmembrane domains of the α_{IIb} subunit of integrin $\alpha_{IIb}\beta_3$. Previously, we demonstrated that these CHAMP peptides bind specifically with reasonable affinity to isolated transmembrane helices of the targeted transmembrane region. These peptides also induced integrin $\alpha_{IIb}\beta_3$ activation due to disruption of the helix−helix interactions between the transmembrane domains of the α_{IIb} and β_3 subunits. In this paper, we show the direct interaction of the designed anti-α_{IIb} CHAMP peptide with isolated full-length integrin $\alpha_{IIb}\beta_3$ in detergent micelles. Further, the behavior of the designed peptides in phospholipid bilayers is essentially identical to their behavior in detergent micelles. In particular, the peptides assume a membrane-spanning α-helical conformation that does not disrupt bilayer integrity. The activity and selectivity of the CHAMP peptides were further explored in platelets, comfirming that anti-α_{IIb} activates wild-type $\alpha_{IIb}\beta_3$ in whole cells as a result of its disruption of the protein−protein interactions between the α and β subunits in the transmembrane regions. These results demonstrate that CHAMP is a successful chemical biology approach that can provide specific tools for probing the transmembrane domains of proteins.

Membrane proteins account for approximately 30% of the entire human proteome; however, studies of their transmembrane (TM)[1] domains have lagged behind due to limitation of their availability, the complexity of the model systems used to study membrane proteins (e.g., micelles, phospholipid vesicles, and bicelles), and, in particular, the lack of exogenous probes with high affinity and specificity (*1*). Conventional antibody-based probing techniques are only useful for water-soluble regions of proteins. Currently, there is no widely used chemical biology method for specifically targeting the TM domains of proteins using exogenous agents.

Computational protein engineering has made major strides (*2*). There are now a variety of methods of designing proteins that recognize water-soluble regions of target proteins (*3*–*6*), but few companion methods for targeting TM regions have been successful. Recently, we reported a general strategy for the computational design of TM domain-targeted peptides, designated the CHAMP (computed helical antimembrane protein) method (*7*). We illustrated the utility of the method by designing peptides that specifically recognize the TM helix of the α subunit of the platelet integrin $\alpha_{IIb}\beta_3$. The TM helices of the α and β subunits of integrin $\alpha_{IIb}\beta_3$ are thought to associate heteromerically in unstimulated platelets and to dissociate following platelet stimulation (*8*–*10*). We showed that anti-α_{IIb}, a peptide designed to target the α_{IIb} TM helix, activated $\alpha_{IIb}\beta_3$ by disrupting the heteromeric $\alpha_{IIb}-\beta_3$ TM helix−helix interaction of the resting integrin (Figure 1). These results illustrate the potential of the CHAMP method for generating high-affinity molecules that bind to and modulate functions of membrane proteins.

In this paper, we validate the specificity of the anti-α_{IIb} CHAMP peptide using biophysical methods to confirm that it recognizes full-length integrin $\alpha_{IIb}\beta_3$ in vitro and in living cells. We found that anti-α_{IIb} selectively binds to the isolated

[†] This work was supported by NIH Grants GM60610, GM54616, HL40387, and HL81012. H.Y. is grateful for financial supports from the University of Colorado, the Association for Research of Childhood Cancer, and the Sidney Kimmel Foundation for Cancer Research (SKF-08-101).

* To whom correspondence should be addressed. E-mail: hang.yin@colorado.edu. Telephone: (303) 492-6786. Fax: (303) 492-5894.

[‡] Department of Biochemistry and Biophysics, University of Pennsylvania School of Medicine.

[§] Current address: Department of Chemistry and Biochemistry, Rowan University, Glassboro, NJ 08028-1701.

[||] Department of Cell and Developmental Biology and Department of Medicine, Hematology-Oncology Division, University of Pennsylvania School of Medicine.

[⊥] University of Colorado.

[1] Abbreviations: ATR-IR, attenuated total reflection infrared; BSA, bovine serum albumin; CHAMP, computed helical antimembrane protein; DMF, dimethylformamide; DMSO, dimethyl sulfoxide; HATU, 2-(1*H*-7-azabenzotriazol-1-yl)-1,1,3,3-tetramethyluronium hexafluorophosphate methanaminium; EDTA, ethylenediaminetetraacetic acid; DPA, dipicolinic acid; FACS, fluorescence-activated cell sorting; FITC, fluorescein isothiocyanate; LDH, lactate dehydrogenase; NMP, *N*-methylpyrrolidine; POPC, 1-palmitoyl-2-oleoyl-*sn*-glycero-3-phosphocholine; POPG, 1-palmitoyl-2-oleoyl-*sn*-glycero-3-[phospho-*rac*-(1-glycerol)]; RBC, human erythrocytes; SDS−PAGE, sodium dodecyl sulfate−polyacrylamide gel electrophoresis; TEM, transmission electron microscopy; TFA, trifluoroacetic acid; TFE, 2,2,2-trifluoroethanol; TM, transmembrane.

10.1021/bi800687h CCC: $40.75
Published on Web 07/22/2008

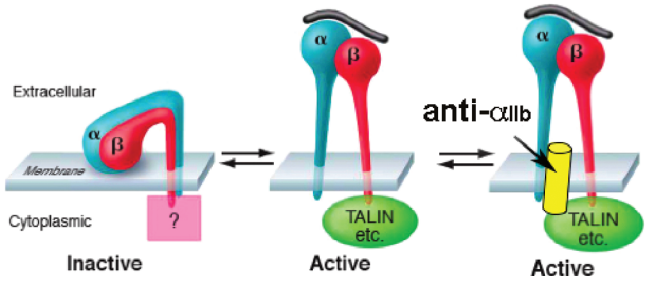

FIGURE 1: Schematic diagram of integrin $\alpha_{IIb}\beta_3$ regulation. Because the α_{IIb} and β_3 subunit TM domains interact when integrins are inactive, any process that destabilizes this interaction would be expected to allow dissociation of the TM domains with concomitant integrin activation. In platelets, this occurs when platelets are stimulated by agonists such as adenosine diphosphate (ADP), inducing binding of the talin phosphotyrosine-binding domain to integrin β_3 subunit cytoplasmic domains (*11*). CHAMP peptides activate platelets by blocking the interactions between the TM helices of the α and β subunits of integrin $\alpha_{IIb}\beta_3$. Extracellular ligands for integrin $\alpha_{IIb}\beta_3$ (e.g., fibrinogen) are shown as black tubes. Question marks indicate unclear interactions.

full-length integrin $\alpha_{IIb}\beta_3$ in detergent micelles and phospholipid bilayers, assumes a membrane-spanning α-helical conformation that does not disrupt the bilayer integrity, and activates $\alpha_{IIb}\beta_3$ by disrupting the association of α_{IIb} and β_3 transmembrane helices. These results support the notion that CHAMP is a general method for designing membrane-spanning peptides targeting protein TM domains.

EXPERIMENTAL PROCEDURES

General Peptide Synthesis. Peptides were synthesized using an Applied Biosystems 430A peptide synthesizer at 0.25 mmol scales. These peptides were synthesized on a Rink Amide AM resin (200−400 mesh) (Nova Biochem) with a substitution level of 0.71 mmol/g. Activation of the free amino acids was achieved with 2-(1*H*-7-azabenzotriazol-1-yl)-1,1,3,3-tetramethyluronium hexafluorophosphate methanaminium (HATU, 0.40 M solution in DMF). The reaction solvent contains 25% DMSO and 75% NMP (HPLC-grade, Aldrich). Side chain deprotection and simultaneous cleavage from the resin were performed using a mixture of trifluoroacetic acid (TFA), thioanisole, 1,2-ethanedithiol, and anisole (90:5:3:3, v/v) at room temperature, under a N_2 flow for 2 h. The crude peptides collected from precipitation with cold diethyl ether (Aldrich) were dissolved in a mixture of 2-propanol, acetonitrile, and water (6:3:1) and then lyophilized overnight. The peptides were then purified on a preparative reverse phase HPLC system (Varian ProStar 210) with a C-4 preparative column (Vydac) using a linear gradient of buffer A (0.1% TFA in Millipore water) and buffer B (6:3:1 2-propanol/acetonitrile/water) containing 0.1% TFA. Elution of the purified peptides occurred at approximately 75% buffer B. The identities of the purified peptides were confirmed by MALDI-TOF mass spectroscopy on a Voyager Biospectrometry Workstation (PerSeptive Biosystems), and their purity was assessed using a HP1100 analytical HPLC system (Hewlett-Packard) with an analytical C-4 column (Vydac) and a linear A/B gradient.

The coumarin label of anti-α_{IIb} and anti-α_{IIb}mut was attached using the standard method (*12*). Two additional glycine residues were coupled to the amino terminus of the peptide resin using standard manual peptide synthesis conditions. The Fmoc protection group was removed with 20% piperidine in DMF. Resin was rinsed with DMF four times, then swelled with dichloromethane, and drained. 7-Hydroxycoumarin-3-carboxylic acid (Anaspec) was dissolved in a pyridine/DMF/DCM mixture (12:7:5) to prepare the 0.1 M solution. The resulting solution was added to the resin. The suspension mixture was stirred at room temperature in the dark until the ninhydrin test indicated that the reaction was complete.

Sodium Dodecyl Sulfate−Polyacrylamide Gel Electrophoresis (SDS−PAGE). Electrophoresis was carried out using precast SDS−polyacrylamide gels (12% NuPAGE 10-well Bis-Tris gels, Invitrogen). The peptide samples were prepared in buffer [10 mM HEPES (pH 7.5), 60 mM *N*-octyl β-D-glucopyranoside, 0.5 mM $CaCl_2$, and 0.02% NaN_3] and incubated overnight. Before electrophoresis, each sample was incubated at 90 °C for 7 min. Electrophoresis was carried out at room temperature with NuPAGE MES SDS running buffer (Invitrogen) at 125 mV for 55 min. The resulting gel was stained using a NOVEX stain kit (Invitrogen).

Fluorescence Anisotropy Assay. The full-length integrin $\alpha_{IIb}\beta_3$ protein in buffer [7.9 mg/mL, 10 mM HEPES (pH 7.5), 60 mM *N*-octyl β-D-glucopyranoside, 0.5 mM $CaCl_2$, and 0.02% NaN_3] is prepared using the previously reported method (*13*). Fluorescence polarization experiments were conducted on an ATF105 spectrofluorometer (Aviv Instruments, Inc.) using a 0.3 cm path length cuvette. Spectra were recorded at 25 °C using 1.0 nm slit widths. Excitation at 408 nm was used for the coumarin-labeled peptide. Anisotropy measurements were recorded upon titration of the integrin $\alpha_{IIb}\beta_3$ protein at varying concentrations into a solution of 64 nM anti-α_{IIb} CHAMP peptide. Data analysis was carried out using a previously described method (*14*).

Attenuated Total Reflection Infrared (ATR-IR) Spectroscopy. ATR-IR spectroscopy was performed as previously described (*15*). Briefly, the purified anti-α_{IIb} peptide was solubilized in a 1:1 (v:v) mixture of 2-propanol and H_2O containing 0.1% HCl, frozen, and lyophilized. This process was repeated for a total of three rounds to remove any TFA salts from the purification process. The anti-α_{IIb} peptide was then solubilized in a 1:1 (v:v) mixture of 2-propanol and H_2O, mixed with an appropriate volume of lipid dissolved in $CHCl_3$, and dried under a stream of N_2. The lipid composition was a mixture of 1-palmitoyl-2-oleoyl-*sn*-glycero-3-phosphocholine (POPC) and 1-palmitoyl-2-oleoyl-*sn*-glycero-3-[phospho-*rac*-(1-glycerol)] (POPG) (7:3 molar ratio). The final peptide:lipid ratio in the sample was 1:50. The dried peptide/lipid film was subjected to high vacuum for 2−3 h to remove any traces of solvent. The film was reconstituted in 5 mM HEPES-buffered D_2O at pH ~7.1 by vigorous vortexing. The peptide/lipid suspension was then extruded 17 times using an Avestin liposofast mini extruder (Avestin Inc.) equipped with two stacked polycarbonate membranes with an average pore diameter of 200 nm. The peptide-containing vesicles were deposited on the ATR crystal, gently spread with a Teflon bar to form a film, and dried under a gentle stream of N_2. Infrared spectra were recorded on a Nicolet 4700 infrared spectrophotometer (Thermo-Electron Corp.) equipped with a DTGS detector, a ZnSe wire-grid polarizer, and a home-built flow chamber to allow a stream of N_2 bubbled through D_2O to flow over the sample during collection. The internal reflection element was

a zinc selenide ATR crystal (80 mm × 20 mm × 3 mm) with an angle of 45° yielding 25 internal reflections. A total of 512 scans at polarizations of 0° and 90° were collected for each sample. Spectra were recorded at 2 cm^{-1} resolution and analyzed using the OMNIC software package for peak deconvolution and area analysis. The helix orientation angle was calculated from the spectra as previously described (*16*) with the exception that the value used in this study for the crystal refractive index was 2.42 (ZnSe).

Dye Release Assay. Lipids were purchased from Avanti Polar Lipids Inc. (Alabaster, AL) and used without further purification. Formation of large unilamellar vesicles with entrapped $Tb(DPA)_3$ was performed as previously described with several modifications (*17*). POPC and POPG dissolved in chloroform were mixed (7:3 mol:mol) with a trace amount of L-3-phosphatidylcholine-1,2-di[^{14}C]oleoyl (Amersham Biosciences). The lipid mixture was initially dried under a stream of N_2 and then further desiccated under vacuum for at least 3 h to remove any residual chloroform. The dried lipid film was then stored under a head of N_2 at −20 °C until it was used. To form liposomes, the lipid film was rehydrated in HBS buffer [10 mM HEPES and 100 mM NaCl (pH 7.1)] containing 5 mM $TbCl_3$ (Molecular Probes, a division of Invitrogen, Carlsbad, CA) and 15 mM 2,6-pyridinedicarboxylic acid (DPA, Sigma-Aldrich, neutralized to pH 7.0) to yield a final lipid concentration of 20 mM (typically a final volume of 0.5 mL was used). The sample was vigorously vortexed for at least 3 min to ensure complete resuspension of the lipid film. The sample was then subjected to seven rounds of freezing in a dry ice/acetone bath and thawed at 37 °C, to increase trapping yield. The sample was then passed 21 times through a Liposofast extruder (Avestin Inc., Ottowa, ON) with two stacked polycarbonate membranes, each with a pore size of 200 nm. Liposomes were then separated from untrapped molecules by gel filtration on a Sepharose CL-2B column [Sigma, 1.0 cm (inside diameter) × 22 cm]. The lipid concentration was calculated by measuring radioactivity in liposome-containing fractions after the column with a comparison to the radioactivity in an aliquot of liposomes that was taken before the gel filtration step. Liposomes were stored at 4 °C and used for up to 1 week after preparation. Each liposome preparation was checked for nonspecific leakage before use by monitoring the fluorescence in the absence of any externally added analytes.

An aliquot of $Tb(DPA)_3$-containing liposomes was added to HBS supplemented with 10 mM EDTA for a final concentration of 20 μM total lipid in a volume of 1700 μL. Samples were allowed to equilibrate for approximately 5 min, at which point initial intensity readings were taken (F_0). Peptides (or controls) were then added to the sample from a concentrated stock in DMSO to yield the desired peptide:lipid ratio and allowed to equilibrate for 10 min with constant stirring, at which point emission intensity was again recorded (F). Leakage was normalized to the fluorescence intensity value for complete vesicle disruption induced by addition of detergent (F_M).

Hemolysis Assay. The hemolytic effects of the anti-α_{IIb} and anti-α_{IIb}mut peptides were tested using a previously described method (*18*). Suspension of human erythrocytes (RBC, 1%) with peptides of different concentrations were incubated in 150 mM sodium chloride and 10 mM Tris buffer (pH 7.0), in the presence or absence of 1 mg/mL bovine serum albumin (BSA). The samples were prepared by combining 400 mL of the RBC suspension and peptide stock solutions (10 mM in DMSO). After incubation at 37 °C for 1 h, the samples were centrifuged at 14000 rpm for 5 min, and the OD_{400} of the supernatant was measured.

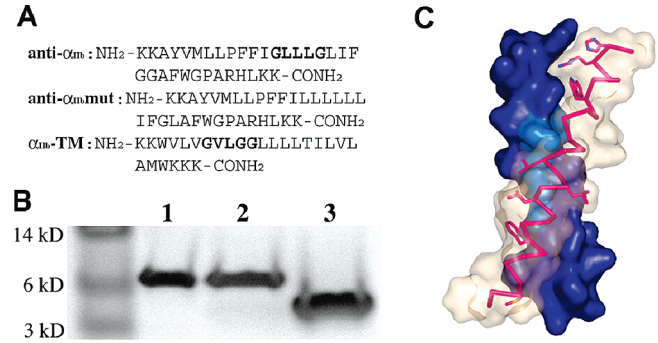

FIGURE 2: (A) Sequences of the anti-α_{IIb} CHAMP peptide, the control peptide anti-α_{IIb}mut, and the targeted α_{IIb}-TM helix. (B) SDS−PAGE of anti-α_{IIb} (lane 1), coumarin-labeled anti-α_{IIb} (lane 2), and anti-α_{IIb}mut (lane 3). (C) Computational model of anti-α_{IIb} bound to the α_{IIb} TM domain. The model predicts that anti-α_{IIb} (red stick) recognizes the "hot spot" on the α_{IIb}-TM binding surface (light blue) with spatial complementarity at the helix-crossing site.

Transmission Electron Microscopy (TEM). Electron microscopy of purified integrin $\alpha_{IIb}\beta_3$ heterodimers was performed as previously described (*19*). We prepared rotary-shadowed samples using a modification of standard procedures (*20*) by spraying a dilute solution of molecules in a volatile buffer (0.05 M ammonium formate) and glycerol (30−50%) onto freshly cleaved mica and shadowing it with tungsten in a vacuum evaporator (Denton Vacuum Co., Cherry Hill, NJ). All specimens were examined in a FEI/Philips 400 electron microscope (Philips Electronic Instruments Co., Mahwah, NJ), operating at 80 kV and at a magnification of 60000×.

Fluorescence-Activated Cell Sorting (FACS). Freshly isolated platelets were added to 200 mg/mL FITC-conjugated fibrinogen and then incubated with 20 μM ADP or 2 μM anti-α_{IIb} CHAMP peptides in the presence or absence of 5 mM EDTA for 3 min at room temperature. After incubation, the platelets were fixed with 0.37% formalin in PBS buffer for 10 min, then washed, and examined by FACS analysis as previously reported (*21*).

RESULTS AND DISCUSSION

Anti-α_{IIb} was prepared using Fmoc solid-state peptide synthesis (SSPS) with HATU as the activating agent to overcome the difficulty of synthesizing membrane-embedded protein sequences (*22*). Double coupling conditions were used at the β-branched amino acid residues. High purity was confirmed by chromatography. A control peptide, anti-α_{IIb}mut, in which the three Gly residues in the "Gly zipper" motif (GXXXGXXXG) were mutated to Leu (*23*), was also synthesized, as was a peptide, designated α_{IIb}-TM, spanning residues Trp968−Lys989 of α_{IIb} (Figure 2A). For binding measurements using fluorescence spectroscopy, we prepared 7-hydroxycoumarin-3-carboxamide-labeled anti-α_{IIb} (coum-anti-α_{IIb}) and anti-α_{IIb}mut (coum-anti-α_{IIb}mut) via a linker to the N-termini of the peptides.

To confirm that the designed CHAMP peptides, as well as its target α_{IIb}-TM, take up structured conformations in artificial membrane systems (detergent micelles) and undergo oligomerization as previously reported in cellular membranes (*7, 24*), we used SDS−PAGE to study the oligomerization state of the free and tagged anti-α_{IIb} peptides as well as anti-α_{IIb}mut. SDS has previously been shown to provide a micellar environment that mimics phospholipid bilayers (*25*). We found that both anti-α_{IIb} (3.7 kDa) and coumarin-labeled anti-α_{IIb} (4.0 kDa) migrated as dimers (Figure 2B), consistent with a previous experiment using the TOXCAT system that measures transmembrane domain interactions in bacterial membranes (*7*). By contrast, anti-α_{IIb}mut migrated as a monomer, which confirmed that the Gly zipper motif is critical for the interhelical recognition. Taken together, these results indicate that detergent micelles are a valid model system for studying CHAMP peptide−target interactions. They also demonstrate that CHAMP peptides have a high propensity to homodimerize, even in the presence of excessive competing detergent molecules.

Previously, we found that anti-α_{IIb} associates with a short peptide (ca. 3 kDa) corresponding to the TM region of the α_{IIb} subunit of integrin $\alpha_{IIb}\beta_3$ in micelles and phospholipid vesicles (*7*). However, $\alpha_{IIb}\beta_3$ is a complex macromolecule (ca. 230 kDa) containing two nonidentical transmembrane domains. To demonstrate that anti-α_{IIb} also binds to the α_{IIb} transmembrane domain in full-length $\alpha_{IIb}\beta_3$, we used fluorescence anisotropy titrations of anti-α_{IIb} to full-length $\alpha_{IIb}\beta_3$ in *N*-octyl β-D-glucopyranoside micelles. The fluorescence anisotropy of a coumarin-labeled peptide in solution correlates with its tumbling and rotational rates (*14*). However, when the coumarin-labeled peptide is bound to a much larger protein, its tumbling is constrained and the level of polarization increases. The advantages of this assay are that it does not require immobilization of either the receptor or the ligand, requires small amounts of peptide and protein as fluorescein has a high quantum yield, and can be readily developed into a high-throughput format. We added increasing amounts of coumarin-labeled anti-α_{IIb} or anti-α_{IIb}mut to a constant concentration of an $\alpha_{IIb}\beta_3$ solution and monitored the resulting polarization increase. Plotting the anisotropy of coum-anti-α_{IIb} as a function of the concentration of $\alpha_{IIb}\beta_3$ revealed a binding isotherm with an apparent K_{diss} of $(1.3 \pm 0.2) \times 10^{-5}$ in mole fraction units, indicating that the peptide also binds tightly to the intact integrin (Figure 3). The control peptide, coum-anti-α_{IIb}mut, displayed an ≈100-fold lower affinity for $\alpha_{IIb}\beta_3$. We also found that coum-anti-α_{IIb} specifically recognized the TM domain of integrin α_{IIb}, but not that of integrin α_v, demonstrating that these CHAMP peptides can differentiate closely relevant homologous integral membrane targets (*7*).

Integrins are inactive when their TM domain-containing stalks are in the proximity of each other and active when the stalks separate (*19, 26*). Consistent with our previous report, transmission electron microscopy (TEM) of purified rotary-shadowed $\alpha_{IIb}\beta_3$ in buffer containing *N*-octyl β-D-glucopyranoside and 1 mM $CaCl_2$ revealed that the majority of inactive $\alpha_{IIb}\beta_3$ molecules had a closed configuration with their stalks touching at the their tips (*19*). By contrast, when anti-α_{IIb} was present, most of the $\alpha_{IIb}\beta_3$ molecules had an open configuration with separated stalks. Statistical analyses indicated that the presence of 5.0 μM anti-α_{IIb} induced the

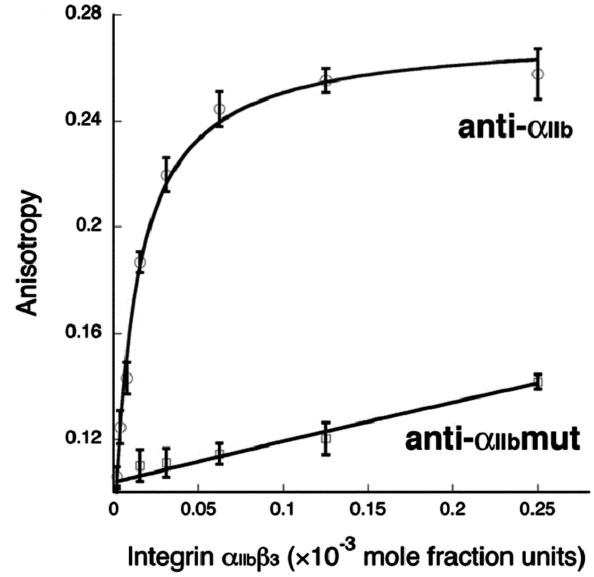

FIGURE 3: Fluorescence polarization titration shows that full-length integrin $\alpha_{IIb}\beta_3$ selectively associates with anti-α_{IIb} over anti-α_{IIb}mut.

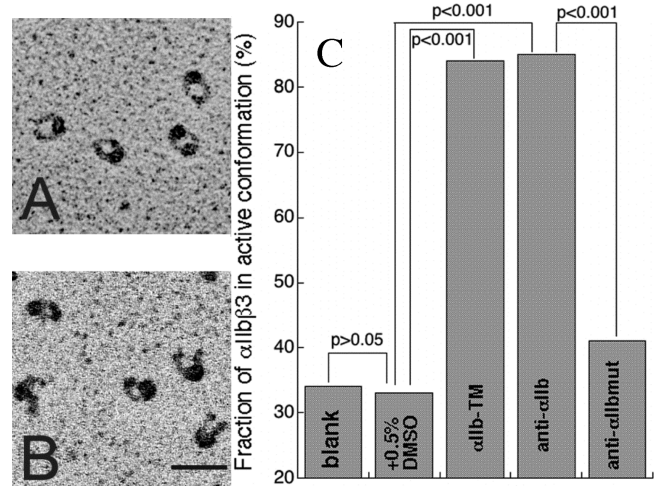

FIGURE 4: Transmission electron microscopy of purified $\alpha_{IIb}\beta_3$ in "closed" (A, in $CaCl_2$-containing buffer alone) and "open" (B, in $CaCl_2$-containing buffer and 3 μM anti-α_{IIb}) forms. Individual $\alpha_{IIb}\beta_3$ molecules were visualized using TEM after rotary shadowing with tungsten (magnification of 170000×; magnification bar = 30 nm). Integrin molecules are found either in the inactive state or in the active state with their transmembrane stalks closed or open, respectively. (C) Statistical analyses of the effects of α_{IIb}-TM, anti-α_{IIb}, and anti-α_{IIb}mut in activating integrin $\alpha_{IIb}\beta_3$.

majority of integrin $\alpha_{IIb}\beta_3$ molecules to convert to their active form (Figure 4). By contrast, anti-α_{IIb}mut induced negligible activation at the same concentrations. These observations are consistent with the notion that anti-α_{IIb} activates $\alpha_{IIb}\beta_3$ by disrupting the TM heterodimer, maintaining the integrin in its inactive state.

To demonstrate that anti-α_{IIb} takes up a membrane-spanning orientation in phospholipid bilayers, we used phospholipid vesicles as the artificial membrane system and polarized attenuated total reflection infrared (ATR-IR) spectroscopy to confirm that anti-α_{IIb} spans the membrane. ATR-IR spectroscopy exploits the fact that in an ordered sample, a given bond will absorb infrared radiation differentially depending on the polarization of the light and the angle at which the bond is oriented relative to the polarized

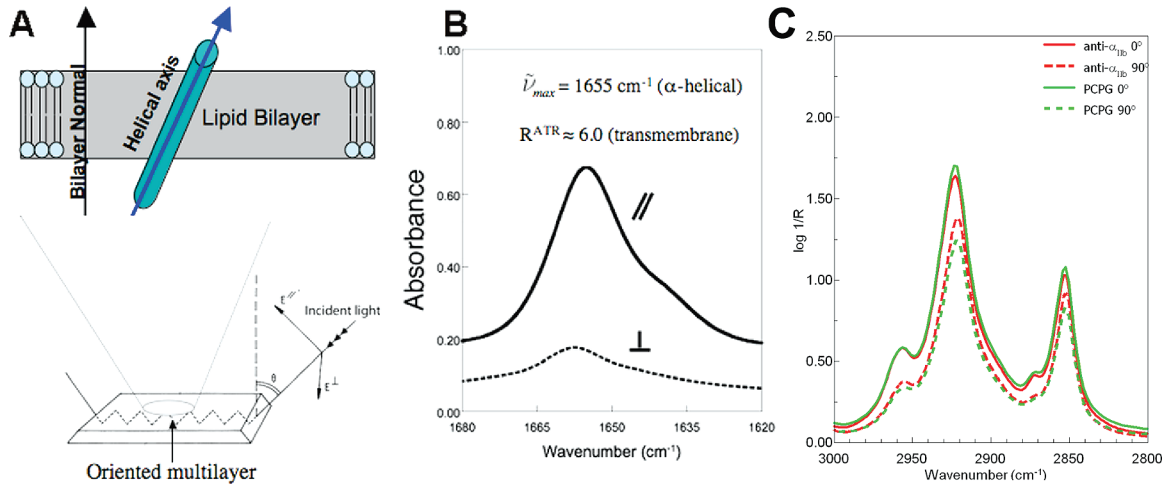

FIGURE 5: ATR-IR. (A) Schematic representation of ATR-IR experiments. The helix angle with respect to the bilayer normal is calculated using the ratio of the amide I absorbance band using 0° and 90° polarized incident radiation, R^{ATR}. (B) ATR-IR spectra collected at 0° (parallel) and 90° (perpendicular) polarized incident radiation. (C) Methylene stretching region of the polarized ATR-IR spectra of POPC/POPG bilayers in the absence (green) and presence (red) of anti-α_{IIb}. The average R^{ATR} for pure POPC/POPG lipid bilayers was ~1.45, while the R^{ATR} for bilayers containing anti-α_{IIb} was ~1.33 (R^{ATR} values are averages of two or three independent samples).

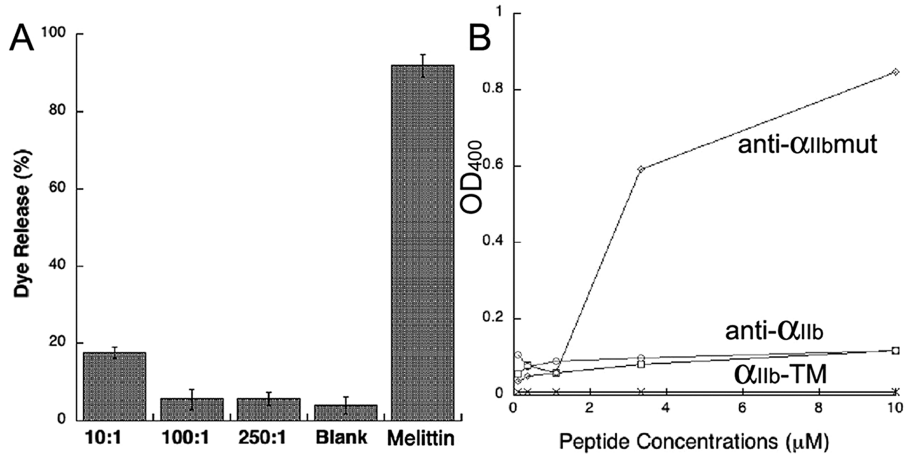

FIGURE 6: Toxicity assays. (A) Dye release induced by anti-α_{IIb}. POPC/POPG (7:3) vesicles containing trapped Tb and DPA were exposed to anti-α_{IIb} at various peptide:lipid ratios or to the known pore-forming peptide melittin. Peptides were incubated with the loaded vesicles for 10 min before fluorescence was measured. Release was quantified using intensity before addition as a baseline (F_0) and fluorescence after the vesicles had been completely disrupted with detergent as a final maximum fluorescence (F_M). (B) Hemolysis induced by the CHAMP peptides. Human erythrocyte hemolysis induced by increasing concentrations of anti-α_{IIb} (○), α_{IIb}-TM (□), and anti-α_{IIb}mut (◇) in 10 mM Tris buffer (pH 7.0) and 1 mg/mL BSA.

light. If the secondary structure of a peptide is known, the dichroic ratio (R^{ATR}) of the amide I absorbance when the incident light is polarized at 0° to the amide I absorbance when the light is polarized at 90° can be used to calculate the angle between the helical axis of the peptide and the bilayer normal. We observed the position of the amide I vibration at 1656 cm^{-1}, indicating that anti-α_{IIb} adopted primarily an α-helical conformation in the POPC/POPG bilayers. This is consistent with the previously published CD data (Figure 5). The R^{ATR} of 4.7 corresponds to an angle of ~20°, indicating that the peptide was inserted nearly perpendicular to the plane of the bilayer. The ~20° angle of insertion is not surprising considering the 33-amino acid length of the peptide, which, if completely helical, would form an α helix of ~49 Å. This is somewhat longer than the hydrophobic thickness of the POPC/POPG bilayer core and could result in the peptide tilting to compensate for the hydrophobic mismatch. The representative spectra of the methylene stretching region of the polarized ATR-IR spectra of POPC/POPG bilayers in the absence and presence of anti-α_{IIb} are shown in Figure 5C. The dichroic ratio (R^{ATR}) values calculated from this region of the spectra are indicative of bilayer ordering, as the major signal arises from the symmetric (~2850 cm^{-1}) and asymmetric (~2920 cm^{-1}) stretching of the CH_2 groups in the lipid acyl chains (*27, 28*). The comparison between the PCPG/PCPG bilayers with and without anti-α_{IIb} showed only a small difference in the dichroic ratios, indicating that the peptide is not significantly disrupting the internal organization of the bilayer or the ability of the bilayers to stack into multilayers on the ZnSe crystal (*27*).

Because amphiphilic peptides can cause cell lysis (*29*), we examined the ability of anti-α_{IIb} to permeabilize phospholipid membranes. Anti-α_{IIb} did not induce significant leakage of a fluorescent metal complex, $Tb(DPA)_3$, from lipid vesicles at a lipid:peptide ratio of up to 10:1, suggesting that the anti-α_{IIb} peptide does not significantly perturb the cell membrane (Figure 6). Further toxicity tests for these compounds were conducted using a lactate dehydrogenase (LDH) release assay. Platelets release LDH when their

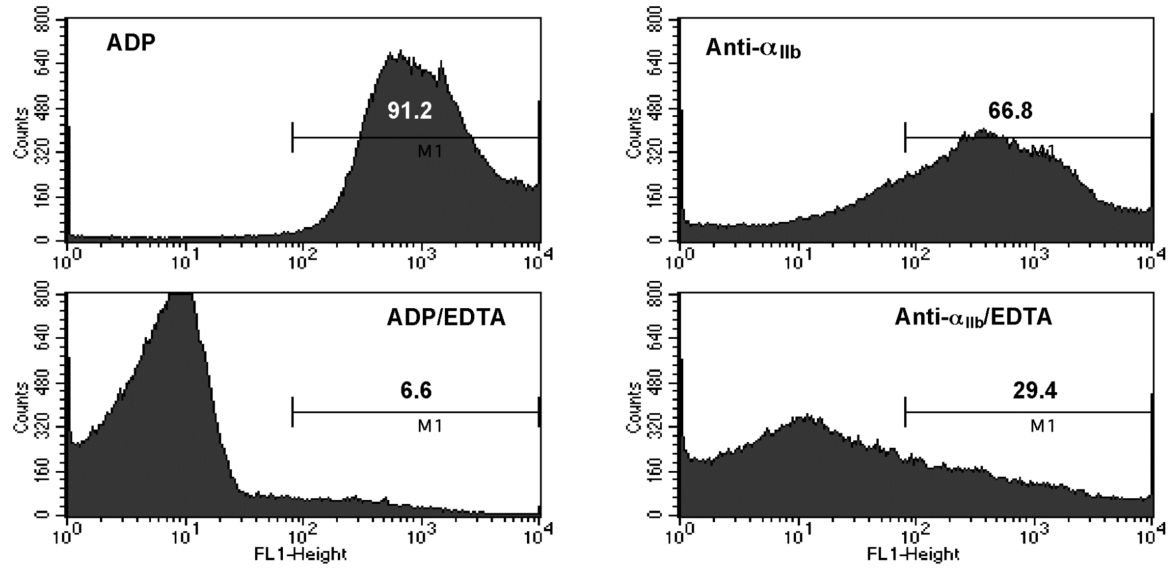

FIGURE 7: Measurement of anti-α_{IIb}-induced binding of FITC-fibrinogen to gel-filtered human platelets by flow cytometry. Fibrinogen binding stimulated by (top left) 20 μM ADP, (top right) 2 μM anti-α_{IIb}, (bottom left) 20 μM ADP in the presence of 5 mM EDTA, and (bottom right) 2 μM anti-α_{IIb} in the presence of 5 mM EDTA. The numbers above M1 represent the percent of analyzed platelets present in the gate.

plasma membrane is perturbed. In the presence of 10 μM anti-α_{IIb}, the level of LDH released by platelets is not significantly higher than the negative control. Moreover, anti-α_{IIb} did not lyse human erythrocyte membranes at concentrations of up to 10 μM.

Agonist-stimulated platelets undergo rapid $\alpha_{IIb}\beta_3$-dependent aggregation in response to agonists such as ADP when the plasma protein fibrinogen binds to the activated conformation of $\alpha_{IIb}\beta_3$ (*30*). To directly demonstrate whether anti-α_{IIb} induces the active conformation of $\alpha_{IIb}\beta_3$ in intact platelets, we used fluorescence-activated cell sorting (FACS) to assess FITC-labeled fibrinogen binding to platelets. The difference in agonist-stimulated fibrinogen binding in the presence and absence of the calcium chelator EDTA indicated the amount of fibrinogen specifically bound to $\alpha_{IIb}\beta_3$. As shown in Figure 7, 2.0 μM anti-α_{IIb} induced $\approx$50% as much specific FITC-fibrinogen binding to platelets as did platelet stimulation by 20 μM ADP. By contrast, anti-α_{IIb}mut exhibited little ability to induce fibrinogen binding to platelets (data not shown). Thus, these data indicate that although it is not as potent as a stimulus at ADP, anti-α_{IIb} does directly enable $\alpha_{IIb}\beta_3$ to bind fibrinogen.

In summary, these results validate the CHAMP method as a successful general chemical biology approach to providing molecular probes with high affinity and specificity for membrane-embedded segments of proteins. In particular, the CHAMP peptide anti-α_{IIb} provides a specific tool for addressing the role of TM domain association in regulating the function of the integrin $\alpha_{IIb}\beta_3$. By blocking the site on the α_{IIb} TM helix that engages the β_3 helix, anti-α_{IIb} activates the integrin, providing strong support for the hypothesis that separation of the helices is required for activation (*10*). CHAMP peptides provide a route to molecules that bind TM regions of their targets, expanding the range of conventional antibody-based methods that can only be applied to water-soluble regions of proteins. Given the current interests involving studying the lateral TM helix associations in membrane protein folding, assembly, and signal transduction (*31*), CHAMP peptides may provide much-needed reagents for probing these processes. Last, although hurdles (such as poor solubility in aqueous solution) associated with the physical properties of the peptides need to be overcome, it is encouraging that engineered peptides from TM helices have shown promise in animal models (*32, 33*). The CHAMP peptides can serve as lead sequences for the development of more druglike, small-molecule peptidomimetic inhibitors of membrane protein−protein interactions, which might ultimately find applications as clinical diagnostics or therapeutics.

REFERENCES

1. Yin, H. (2008) Exogenous Agents that Target Transmembrane Domains of Proteins. *Angew. Chem., Int. Ed. 47*, 2744–2752.
2. Kang, S. G., and Saven, J. G. (2007) Computational protein design: Structure, function and combinatorial diversity. *Curr. Opin. Chem. Biol. 11*, 329–334.
3. Kortemme, T., and Baker, D. (2004) Computational design of protein-protein interactions. *Curr. Opin. Chem. Biol. 8*, 91–97.
4. Shifman, J. M., and Mayo, S. L. (2003) Exploring the origins of binding specificity through the computational redesign of calmodulin. *Proc. Natl. Acad. Sci. U.S.A. 100*, 13274–13279.
5. Reina, J., Lacroix, E., Hobson, S. D., Fernandez-Ballester, G., Rybin, V., Schwab, M. S., Serrano, L., and Gonzalez, C. (2002) Computer-aided design of a PDZ domain to recognize new target sequences. *Nat. Struct. Biol. 9*, 621–627.
6. Ogihara, N. L., Ghirlanda, G., Bryson, J. W., Gingery, M., DeGrado, W. F., and Eisenberg, D. (2001) Design of three-dimensional domain-swapped dimers and fibrous oligomers. *Proc. Natl. Acad. Sci. U.S.A. 98*, 1404–1409.
7. Yin, H., Slusky, J. S., Berger, B. W., Walters, R. S., Vilaire, G., Litvinov, R. I., Lear, J. D., Caputo, G. A., Bennett, J. S., and DeGrado, W. F. (2007) Computational design of peptides that target transmembrane helices. *Science 315*, 1817–1822.
8. Partridge, A. W., Liu, S. C., Kim, S., Bowie, J. U., and Ginsberg, M. H. (2005) Transmembrane domain helix packing stabilizes integrin $\alpha_{IIb}\beta_3$ in the low affinity state. *J. Biol. Chem. 280*, 7294–7300.
9. Luo, B. H., Springer, T. A., and Takagi, J. (2004) A specific interface between integrin transmembrane helices and affinity for ligand. *PLoS Biol. 2*, 776–786.
10. Li, W., Metcalf, D. G., Gorelik, R., Li, R. H., Mitra, N., Nanda, V., Law, P. B., Lear, J. D., DeGrado, W. F., and Bennett, J. S. (2005) A push-pull mechanism for regulating integrin function. *Proc. Natl. Acad. Sci. U.S.A. 102*, 1424–1429.

11. Wegener, K. L., Partridge, A. W., Han, J., Pickford, A. R., Liddington, R. C., Ginsberg, M. H., and Campbell, I. D. (2007) Structural basis of integrin activation by talin. *Cell 128*, 171–182.
12. http://www.anaspec.com.
13. Weisel, J. W., Nagaswami, C., Vilaire, G., and Bennett, J. S. (1992) Examination of the platelet membrane glycoprotein IIb-IIIa complex and its interaction with fibrinogen and other ligands by electron microscopy. *J. Biol. Chem. 267*, 16637–16643.
14. Yin, H., Lee, G. I., Park, H. S., Payne, G. A., Rodriguez, J. M., Sebti, S. M., and Hamilton, A. D. (2005) Terphenyl-based helical mimetics that disrupt the p53/HDM2 interaction. *Angew. Chem., Int. Ed. 44*, 2704–2707.
15. Caputo, G. A., and London, E. (2003) Cumulative effects of amino acid substitutions and hydrophobic mismatch upon the transmembrane stability and conformation of hydrophobic α-helices. *Biochemistry 42*, 3275–3285.
16. Arkin, I. T., MacKenzie, K. R., and Brunger, A. T. (1997) Site-directed dichroism as a method for obtaining rotational and orientational constraints for oriented polymers. *J. Am. Chem. Soc. 119*, 8973–8980.
17. Heuck, A. P., Tweten, R. K., and Johnson, A. E. (2003) Assembly and topography of the prepore complex in cholesterol-dependent cytolysins. *J. Biol. Chem. 278*, 31218–31225.
18. Liu, D., and DeGrado, W. F. (2001) De novo design, synthesis, and characterization of antimicrobial β-peptides. *J. Am. Chem. Soc. 123*, 7553–7559.
19. Litvinov, R. I., Nagaswami, C., Vilaire, G., Shuman, H., Bennett, J. S., and Weisel, J. W. (2004) Functional and structural correlations of individual $\alpha_{IIb}\beta_3$ molecules. *Blood 104*, 3979–3985.
20. Weisel, J. W., Stauffacher, C. V., Bullitt, E., and Cohen, C. (1985) A model for fibrinogen: Domains and sequence. *Science 230*, 1388–1391.
21. Basani, R. B., D'Andrea, G., Mitra, N., Vilaire, G., Richberg, M., Kowalska, M. A., Bennett, J. S., and Poncz, M. (2001) RGD-containing peptides inhibit fibrinogen binding to platelet $\alpha_{IIb}\beta_3$ by inducing an allosteric change in the amino-terminal portion of α_{IIb}. *J. Biol. Chem. 276*, 13975–13981.
22. Fisher, L. E., and Engelman, D. M. (2001) High-yield synthesis and purification of an α-helical transmembrane domain. *Anal. Biochem. 293*, 102–108.
23. Kim, S., Jeon, T. J., Oberai, A., Yang, D., Schmidt, J. J., and Bowie, J. U. (2005) Transmembrane glycine zippers: Physiological and pathological roles in membrane proteins. *Proc. Natl. Acad. Sci. U.S.A. 102*, 14278–14283.
24. Yin, H., Litvinov, R. I., Vilaire, G., Zhu, H., Li, W., Caputo, G. A., Moore, D. T., Lear, J. D., Weisel, J. W., Degrado, W. F., and Bennett, J. S. (2006) Activation of platelet $\alpha_{IIb}\beta_3$ by an exogenous peptide corresponding to the transmembrane domain of α_{IIb}. *J. Biol. Chem. 281*, 36732–36741.
25. DeGrado, W. F., Gratkowski, H., and Lear, J. D. (2003) How do helix-helix interactions help determine the folds of membrane proteins? Perspectives from the study of homo-oligomeric helical bundles. *Protein Sci. 12*, 647–665.
26. Kim, M., Carman, C. V., and Springer, T. A. (2003) Bidirectional transmembrane signaling by cytoplasmic domain separation in integrins. *Science 301*, 1720–1725.
27. Torrecillas, A., Martínez-Senac, M. M., Goormaghtigh, E., de Godos, A., Corbalán-García, S., and Gómez-Fernández, J. C. (2005) Modulation of the membrane orientation and secondary structure of the C-terminal domains of Bak and Bcl-2 by lipids. *Biochemistry 44*, 10796–10809.
28. Goormaghtigh, E., Raussens, V., and Ruysschaert, J. M. (1999) Attenuated total reflection infrared spectroscopy of proteins and lipids in biological membranes. *Biochim. Biophys. Acta 1422*, 105–185.
29. Bechinger, B. (1997) Structure and functions of channel-forming peptides: Magainins, cecropins, melittin and alamethicin. *J. Membr. Biol. 156*, 197–211.
30. Bennett, J. S. (2001) Novel platelet inhibitors. *Annu. Rev. Med. 52*, 161–184.
31. Senes, A., Engel, D. E., and DeGrado, W. F. (2004) Folding of helical membrane proteins: The role of polar, GXXXG-like and proline motifs. *Curr. Opin. Struct. Biol. 14*, 465–479.
32. Manolios, N., Collier, S., Taylor, J., Pollard, J., Harrison, L. C., and Bender, V. (1997) T-Cell antigen receptor transmembrane peptides modulate T-cell function and T cell-mediated disease. *Nat. Med. 3*, 84–88.
33. Gerber, D., Quintana, F. J., Bloch, I., Cohen, I. R., and Shai, Y. (2005) D-Enantiomer peptide of the TCRα transmembrane domain inhibits T-cell activation in vitro and in vivo. *FASEB J. 19*, 1190–1192.

BI800687H